2010 American Control Conference
Marriott Waterfront, Baltimore, MD, USA
June 30-July 02, 2010

Preventing transition to turbulence using streamwise traveling waves: theoretical analysis

Rashad Moarref and Mihailo R. Jovanović

Abstract— **We assess the efficacy of a zero-net-mass-flux blowing and suction in the form of streamwise traveling waves for controlling the onset of turbulence in a channel flow. For small amplitude actuation along the walls, we utilize perturbation analysis to determine modifications in the base flow and to examine the resulting net power balance. Sensitivity of the velocity fluctuations around this base flow is then employed as a basis for selection of traveling wave parameters. Our simulation-free approach reveals that, relative to the uncontrolled flow, the velocity fluctuations around the upstream traveling waves at best exhibit similar sensitivity to background disturbances. In contrast, the downstream traveling waves with properly designed speed and frequency can significantly reduce sensitivity which makes them well-suited for preventing transition. These theoretical predictions are facilitated by perturbation analysis (in the wave amplitude) of the linearized Navier-Stokes equations, and they are verified using full-scale simulations of the nonlinear flow dynamics in companion paper, [1].**

Index Terms— **Flow control; spatially-periodic systems; traveling waves; turbulence suppression; variance amplification.**

I. Introduction

Fluid motion is usually classified as either laminar or turbulent; flows that are smooth and ordered (laminar) may become complex and disordered (turbulent) as the flow strength increases. This process is commonly referred to as transition (to turbulence). A laminar flow is characterized by smaller viscous shear stresses and velocity gradients than a turbulent flow, leading to a lower skin-friction drag force on a vehicle moving through a fluid in the laminar regime.

Sensorless flow control represents a viable and effective alternative to strategies with wall-mounted arrays of sensors and actuators. In [2], direct numerical simulations (DNS) of the Navier-Stokes (NS) equations were used to show that a surface blowing and suction in the form of an upstream traveling wave (UTW) results in a sustained sublaminar drag. A fundamental limitation on the balance of power in transpiration-based techniques was recently examined in [3]; this study showed that, relative to the uncontrolled laminar flow, any strategy that results in sublaminar drag necessarily has negative net efficiency.

In this paper, we show that a positive net efficiency can be achieved in a channel flow subject to streamwise traveling waves if the uncontrolled flow becomes turbulent but the controlled flow stays laminar. Starting from this observation, we develop a framework for selection of control parameters that are capable of (i) improving dynamical properties of the flow; and (ii) achieving positive net efficiency. Our main analytical tool is input-output analysis of stochastically forced linearized NS equations with spatially periodic coefficients. Periodicity in the problem arises from the base flow induced by the traveling waves and it introduces significant design challenges. Motivated by our desire to have low cost of control we confine our study to flows subject to small amplitude traveling waves. This also facilitates use of efficient perturbation-analysis-based techniques that provide an explicit formula for variance amplification of velocity fluctuations. Our approach shows that the UTWs are poor candidates for preventing transition; conversely, perturbation analysis reveals that *properly designed* downstream traveling waves (DTWs) can substantially reduce amplification of the most energetic flow structures. This indicates that the DTWs can be used as an effective means for preventing transition. Moreover, we show the existence of DTW parameters that result in a positive net efficiency compared to the uncontrolled flow that becomes turbulent. Our theoretical predictions are confirmed in [1], where we exhibit the predictive power of the proposed method by conducting high fidelity simulations of the nonlinear flow equations.

Our presentation is organized as follows: in § II, we formulate the governing equations in the presence of traveling waves; the influence of blowing and suction along the walls on the nominal skin-friction drag coefficient and the nominal net efficiency is also discussed in this section. A frequency representation of the NS equations linearized around velocity induced by traveling waves is presented in § III. We further discuss a notion of variance amplification (i.e., the H_2 norm) for spatially-periodic systems and present an analytical approach to determining the H_2 norm in flows subject to small amplitude traveling waves. In § IV, we employ perturbation analysis to identify the values of wave frequency and speed that reduce variance amplification relative to the uncontrolled flow; we show that all amplification trends are captured by perturbation analysis up to a second order in wave amplitude. A brief summary of the main results is provided in § V.

II. Problem formulation

A. Governing equations

Consider a channel flow (cf. Fig. 1 for illustration) governed by the non-dimensional incompressible NS equations

$$\mathbf{u}_{\bar{t}} = -(\mathbf{u}\cdot\boldsymbol{\nabla})\,\mathbf{u} - \boldsymbol{\nabla}\mathrm{P} + (1/R_c)\Delta\mathbf{u} + \mathbf{F},\quad 0 = \boldsymbol{\nabla}\cdot\mathbf{u}, \tag{1}$$

with the Reynolds number defined in terms of the centerline velocity of the parabolic laminar profile U_c and channel half-

R. Moarref and M. R. Jovanović are with the Department of Electrical and Computer Engineering, University of Minnesota, Minneapolis, MN 55455, USA (e-mails: rashad@umn.edu, mihailo@umn.edu).

Financial support from the National Science Foundation under CAREER Award CMMI-06-44793 is gratefully acknowledged.

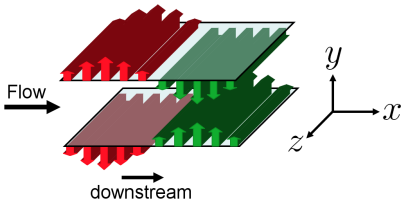

Fig. 1. A channel flow with blowing and suction along the walls.

height δ, $R_c = U_c\,\delta/\nu$. The kinematic viscosity is denoted by ν, the velocity vector is given by $\mathbf{u}$, P is the pressure, $\mathbf{F}$ is the body force, $\boldsymbol{\nabla}$ is the gradient, and $\Delta = \boldsymbol{\nabla}\cdot\boldsymbol{\nabla}$ is the Laplacian. The spatial coordinates and time are represented by $(\bar{x}, \bar{y}, \bar{z})$ and $\bar{t}$, respectively.

In addition to a constant pressure gradient, $P_{\bar{x}}$, the flow is exposed to a zero-net-mass-flux surface blowing and suction in the form of a streamwise traveling wave. In the absence of the nominal body force, $\bar{\mathbf{F}} \equiv 0$, base velocity $\mathbf{u}_b = (U, V, W)$ represents the steady-state solution to (1) subject to

$$\begin{aligned} V(\bar{y} = \pm 1) &= \mp 2\,\alpha\,\cos\left(\omega_x(\bar{x} - c\,\bar{t})\right), \quad \bar{\mathbf{F}} \equiv 0, \\ U(\pm 1) &= V_{\bar{y}}(\pm 1) = W(\pm 1) = 0, \quad P_{\bar{x}} = -2/R_c, \end{aligned} \tag{2}$$

where ω_x, c, and α, respectively, identify frequency, speed, and amplitude of the streamwise traveling wave. Positive values of c define a DTW, whereas negative values of c define a UTW. The time dependence in $V(\pm 1)$ can be eliminated by the transformation, $(x = \bar{x} - c\bar{t},\ y = \bar{y},\ z = \bar{z},\ t = \bar{t})$. This change of coordinates does not influence the spatial differential operators, but it transforms the time derivative to $\partial_{\bar{t}} = \partial_t - c\,\partial_x$, which adds an additional convective term to the NS equations

$$\begin{aligned} \mathbf{u}_t &= c\mathbf{u}_x - (\mathbf{u}\cdot\boldsymbol{\nabla})\,\mathbf{u} - \boldsymbol{\nabla}\mathrm{P} + (1/R_c)\Delta\mathbf{u} + \mathbf{F}, \\ 0 &= \boldsymbol{\nabla}\cdot\mathbf{u}. \end{aligned} \tag{3}$$

In new coordinates, the wall-actuation (2) induces a two-dimensional base velocity, $\mathbf{u}_b = (U(x,y), V(x,y), 0)$, which represents the steady-state solution to (3).

The equations describing dynamics (up to a first order) of velocity fluctuations $\mathbf{v} = (u, v, w)$ around base velocity, $\mathbf{u}_b$, are obtained by decomposing each field in (3) into the sum of base and fluctuating parts, i.e., $\{\mathbf{u} = \mathbf{u}_b + \mathbf{v},\ \mathrm{P} = P + p,\ \mathbf{F} = 0 + \mathbf{d}\}$, and by neglecting the quadratic term in $\mathbf{v}$

$$\begin{aligned} \mathbf{v}_t &= c\mathbf{v}_x - (\mathbf{u}_b\cdot\boldsymbol{\nabla})\,\mathbf{v} - (\mathbf{v}\cdot\boldsymbol{\nabla})\,\mathbf{u}_b - \boldsymbol{\nabla}p + \\ &\quad (1/R_c)\Delta\mathbf{v} + \mathbf{d}, \quad 0 = \boldsymbol{\nabla}\cdot\mathbf{v}. \end{aligned} \tag{4}$$

Note that the boundary conditions (2) are satisfied by base velocity and, thus, velocity fluctuations assume homogeneous Dirichlet boundary conditions.

B. Base flow

We consider the situation in which a surface blowing and suction has a small amplitude α. In this case, a perturbation analysis can be employed to efficiently solve (3) subject to (2) and determine the corrections to the base parabolic profile. Up to a second order in α, $U(x,y)$ and $V(x,y)$ can be represented as

$$\begin{aligned} U(x,y) &= U_0(y) + \alpha\,U_1(x,y) + \alpha^2\,U_2(x,y) + \mathcal{O}(\alpha^3), \\ V(x,y) &= \alpha\,V_1(x,y) + \alpha^2\,V_2(x,y) + \mathcal{O}(\alpha^3), \end{aligned}$$

where $U_0(y) = 1 - y^2$ denotes base velocity in flow with no control. Owing to the spatially periodic boundary conditions, the corrections to the base velocity in flow subject to traveling waves inherit periodicity in the streamwise direction

$$\begin{aligned} U_1(x,y) &= U_{1,-1}(y)\,\mathrm{e}^{-\mathrm{i}\omega_x x} + U_{1,1}(y)\,\mathrm{e}^{\mathrm{i}\omega_x x}, \\ V_1(x,y) &= V_{1,-1}(y)\,\mathrm{e}^{-\mathrm{i}\omega_x x} + V_{1,1}(y)\,\mathrm{e}^{\mathrm{i}\omega_x x}, \\ U_2(x,y) &= U_{2,0}(y) + U_{2,-2}(y)\,\mathrm{e}^{-2\mathrm{i}\omega_x x} + U_{2,2}(y)\,\mathrm{e}^{2\mathrm{i}\omega_x x}, \\ V_2(x,y) &= V_{2,-2}(y)\,\mathrm{e}^{-2\mathrm{i}\omega_x x} + V_{2,2}(y)\,\mathrm{e}^{2\mathrm{i}\omega_x x}. \end{aligned}$$

The nominal bulk flux is determined by $U_B = (1/2)\int_{-1}^{1}\overline{U}(y)\,\mathrm{d}y$ where the overline denotes average over horizontal directions. The nominal flux in the uncontrolled flow is $U_{B,0} = (1/2)\int_{-1}^{1}U_0(y)\,\mathrm{d}y = 2/3$. Even in the absence of driving pressure gradient, it was recently shown that blowing and suction along the walls induces 'pumping' in a direction opposite to that of the traveling wave [4].

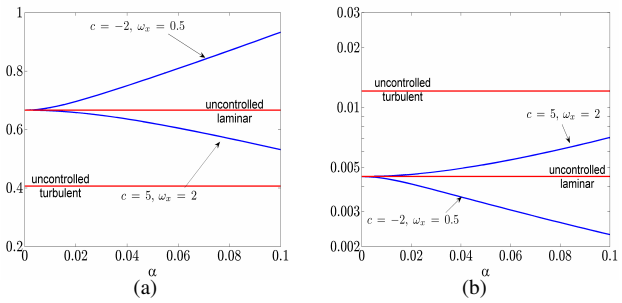

Fig. 2. (a) The nominal flux, $U_B(\alpha)$; and (b) the nominal skin-friction drag coefficient, $C_f(\alpha)$, for a UTW and a DTW in channel flow with $R_c = 2000$. The results are obtained by solving (3) subject to (2), at the steady-state, using Newton iterations; U_B and C_f of the laminar and turbulent uncontrolled flows are also shown for comparison.

Fig. 2 is obtained by solving (3) subject to (2), at the steady-state, using Newton's method. The nominal flux and associated drag coefficient for a UTW with $c = -2$ and $\omega_x = 0.5$ and a DTW with $c = 5$ and $\omega_x = 2$ are shown. The flux and drag coefficient of both laminar and turbulent uncontrolled flows are also given for comparison. The nominal skin-friction drag coefficient is defined as

$$C_f = 2\,\overline{\tau}_w/U_B^2 = -2\,P_x/U_B^2,$$

where $\overline{\tau}_w$ is the nondimensional average wall-shear stress. For the fixed pressure gradient, $P_x = -2/R_c$, the nominal skin-friction drag coefficient is inversely proportional to square of the nominal flux and, in uncontrolled laminar flow with $R_c = 2000$, we have $C_f = 4.5 \times 10^{-3}$. The UTWs produce larger nominal flux (and, consequently, smaller nominal drag coefficient) compared to both laminar and turbulent uncontrolled flows. On the other hand, the DTWs yield smaller nominal flux (and, consequently, larger nominal drag coefficient) compared to uncontrolled laminar flow. In situations where uncontrolled flow becomes turbulent,

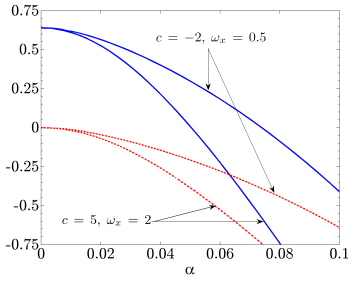

Fig. 3. The steady-state net efficiency, Π_{net}, as a function of control amplitude α for a UTW with $(c = -2,\ \omega_x = 0.5)$ and a DTW with $(c = 5,\ \omega_x = 2)$ at $R_c = 2000$. The results are obtained by *assuming* two different scenarios: (i) both the uncontrolled and controlled flows remain laminar (dashed); and (ii) the uncontrolled flow becomes turbulent while the controlled flow stays laminar (solid).

however, the DTWs with amplitudes smaller than a certain threshold value may have lower nominal drag coefficient than the uncontrolled (turbulent) flow.

C. Net efficiency

For the fixed pressure gradient, the difference between the fluxes of the controlled and the uncontrolled flows results in production of a driving power (per unit horizontal area of the channel)

$$\Pi_{prod} \;=\; -2P_x\,(U_{B,c} \,-\, U_{B,u}),$$

where $U_{B,c}$ and $U_{B,u}$ are the nominal flux of the controlled and uncontrolled flows, respectively. On the other hand, the required control power exerted at the walls (per unit horizontal area of the channel) is given by [5]

$$\Pi_{req} \;=\; \overline{VP}\big|_{y=-1} \,-\, \overline{VP}\big|_{y=1}\,. \tag{5}$$

The control net efficiency is determined by the difference of the produced and required powers [6]

$$\%\Pi_{net} \;=\; \Pi_{net}/\Pi_u,\quad \Pi_{net} \;=\; \Pi_{prod} \,-\, \Pi_{req},$$

where $\%\Pi_{net}$ signifies the net power gained (positive Π_{net}) or lost (negative Π_{net}), in the presence of wall-control, in fraction of the power required to drive the uncontrolled flow, $\Pi_u = -2P_x\,U_{B,u}$.

D. Nominal efficiency of laminar controlled flows

Broadly speaking, for the fixed value of the Reynolds number, three cases can be distinguished depending on the energy of background disturbances: (i) both the uncontrolled and the properly designed controlled flows remain laminar (*small* disturbance energy); (ii) the uncontrolled flow becomes turbulent, while the controlled flow stays laminar for the appropriate choice of traveling wave parameters (*moderate* disturbance energy); and (iii) both the uncontrolled and controlled flows become turbulent for all traveling wave parameters (*large* disturbance energy). We note, however, that *poorly* designed traveling waves can promote turbulence even for background disturbances for which the uncontrolled flow stays laminar (see [1]). Fig. 3 shows how much control net efficiency can be achieved at the steady-state for two sets of UTWs and DTWs; the dashed lines are obtained by *assuming* that case (i) holds, and the solid lines are obtained by *assuming* that case (ii) holds. If the uncontrolled flow stays laminar (case (i)), the net efficiency is negative for both UTWs and DTWs. Thus, the uncontrolled laminar flow is more efficient than either a UTW or a DTW laminar flow; this is in agreement with a recent study of [3] where it was shown that any transpiration-based control strategy that results in a sublaminar drag necessarily has negative net efficiency relative to the uncontrolled laminar flow.

On the other hand, in case (ii), the positive net efficiency can be achieved for control amplitudes smaller than a certain threshold value (cf. Fig. 3). For the uncontrolled flow that becomes turbulent, we have $U_{B,u} = 0.4066$ which corresponds to the skin-friction drag coefficient $C_f = 0.0121$ of the uncontrolled turbulent flow (see DNS results of [1]). Owing to the difference between $U_{B,u}$ and $U_{B,0}$, it is possible to obtain a positive net efficiency for sufficiently small value of α. In a nutshell, the control amplitude needs to be large enough to maintain the laminar flow but increasing the control amplitude beyond certain value brings the efficiency down and eventually leads to negative efficiency. If the efficiency is negative, the reduced drag obtained by preventing transition does not lead to any net benefit in the presence of control. However, such controls may be advantageous when the primal interest is in maintaining a laminar flow.

The solid curves in Fig. 3 are computed under the assumption that the uncontrolled flow becomes turbulent while the controlled flow stays laminar. Whether or not the controlled flow can stay laminar depends on the dynamics of velocity fluctuations around streamwise traveling waves.

III. Dynamics of velocity fluctuations

A. Evolution model with forcing

A standard conversion of (4) to the wall-normal velocity (v)/vorticity (η) formulation removes the pressure from the equations and yields the following evolution model

$$\begin{aligned} E\,\boldsymbol{\psi}_t(x,y,z,t) \;&=\; F\,\boldsymbol{\psi}(x,y,z,t) \;+\; G\,\mathbf{d}(x,y,z,t),\\ \mathbf{v}(x,y,z,t) \;&=\; C\,\boldsymbol{\psi}(x,y,z,t). \end{aligned} \tag{6}$$

This model is driven by the body force fluctuation vector $\mathbf{d} = (d_1,\, d_2,\, d_3)$, which can account for flow disturbances. The internal state of (6) is determined by $\boldsymbol{\psi} = (v,\, \eta)$, with Dirichlet and Neumann boundary conditions on v and Dirichlet boundary conditions on η. All operators in (6) are matrices of differential operators in three coordinate directions x, y, and z. While operators E, G, and C do not depend on the base velocity, operator F is base velocity dependent and, hence, it determines changes in the dynamics owing to changes in $\mathbf{u}_b$. Moreover, for base velocity of § II-B, F inherits spatial periodicity in x from $\mathbf{u}_b$ and it can be represented as

$$F \;=\; F_0 \;+\; \sum_{l\,=\,1}^{\infty} \alpha^l \sum_{r\,\overset{2}{=}\,-l}^{l} \mathrm{e}^{\mathrm{i}r\omega_x x} F_{l,r},$$

where F_0 and $F_{l,r}$ are spatially invariant operators in the streamwise and spanwise directions and $\sum_{r\,\overset{2}{=}\,-l}^{l}$ signifies that r takes the values $\{-l, -l+2, \ldots, l-2, l\}$. This

expansion effectively isolates spatially invariant and spatially periodic parts of operator F, which is particularly well-suited for representation of (6) in the frequency domain.

B. Frequency representation of the linearized model

Owing to the structure of the linearized NS equation, the differential operators E, G, and C are invariant with respect to translations in horizontal directions. On the other hand, operator F is invariant in z and periodic in x. Thus, the Fourier transform in z can be applied to algebraize the spanwise differential operators. In other words, the normal modes in z are the spanwise waves $\mathrm{e}^{\mathrm{i}k_z z}$, where k_z denotes the spanwise wavenumber. On the other hand, the appropriate normal modes in x are given by the so-called *Bloch waves* [7], which are determined by a product of $\mathrm{e}^{\mathrm{i}\theta x}$ and the $2\pi/\omega_x$ periodic function in x, with $\theta \in [0,\, \omega_x)$. Based on the above, each signal in (6) (for example, $\mathbf{d}$) can be expressed as

$$\begin{aligned}\mathbf{d}(x,y,z,t) &= \mathrm{e}^{\mathrm{i}k_z z}\mathrm{e}^{\mathrm{i}\theta x}\,\bar{\mathbf{d}}(x,y,k_z,t),\\ \bar{\mathbf{d}}(x,y,k_z,t) &= \bar{\mathbf{d}}(x+2\pi/\omega_x,y,k_z,t),\end{aligned}$$

where $k_z \in \mathbb{R}$, $\theta \in [0,\, \omega_x)$, and only real parts are to be used for representation of physical quantities. Expressing $\bar{\mathbf{d}}(x,y,k_z,t)$ in Fourier series yields

$$\mathbf{d}(x,y,z,t) \;=\; \sum_{n=-\infty}^{\infty} \bar{\mathbf{d}}_n(y,k_z,t)\,\mathrm{e}^{\mathrm{i}(\theta_n x + k_z z)}, \qquad (7)$$

where $\theta_n = \theta + n\omega_x$, and $\{\bar{\mathbf{d}}_n(y,k_z,t)\}_{n\in\mathbb{Z}}$ are the coefficients in the Fourier series expansions of $\bar{\mathbf{d}}(x,y,k_z,t)$.

The frequency representation of the linearized NS equation is obtained by substituting (7) into (6)

$$\begin{aligned}\partial_t \boldsymbol{\psi}_\theta(y,k_z,t) &= \mathcal{A}_\theta(k_z)\boldsymbol{\psi}_\theta(y,k_z,t) + \mathcal{B}_\theta(k_z)\mathbf{d}_\theta(y,k_z,t),\\ \mathbf{v}_\theta(y,k_z,t) &= \mathcal{C}_\theta(k_z)\,\boldsymbol{\psi}_\theta(y,k_z,t).\end{aligned} \qquad (8)$$

This representation is parameterized by k_z and θ and $\boldsymbol{\psi}_\theta(y,k_z,t)$ denotes a bi-infinite column vector, $\boldsymbol{\psi}_\theta(y,k_z,t) = \mathrm{col}\,\{\boldsymbol{\psi}(\theta_n,y,k_z,t)\}_{n\in\mathbb{Z}}$. The same definition applies to $\mathbf{d}_\theta(y,k_z,t)$ and $\mathbf{v}_\theta(y,k_z,t)$. On the other hand, for each k_z and θ, $\mathcal{A}_\theta(k_z)$, $\mathcal{B}_\theta(k_z)$, and $\mathcal{C}_\theta(k_z)$ are bi-infinite matrices whose elements are one-dimensional integro-differential operators in y. The structure of these operators depends on frequency representation of E, F, G, and C in (6). In short, $\mathcal{B}_\theta(k_z)$ and $\mathcal{C}_\theta(k_z)$ are block-diagonal operators and $\mathcal{A}_\theta = \mathcal{A}_{0\theta} + \sum_{l=1}^{\infty}\alpha^l\,\mathcal{A}_{l\theta}$, where $\mathcal{A}_{0\theta}$ and $\mathcal{A}_{l\theta}$ are structured operators. The particular structure of $\mathcal{A}_{0\theta}$ and $\mathcal{A}_{l\theta}$ is exploited in perturbation analysis of the H_2 norm for small α in § III-D.

C. H_2 norm of the linearized model

The frequency representation (8) contains a large amount of information about linearized dynamics. For example, it can be used to assess stability properties of the underlying base flow. However, since the early stages of transition in wall-bounded shear flows are not appropriately described by the stability properties of the linearized equations [8], we perform an input-output analysis of stochastically forced model (8) to assess the effectiveness of the proposed control strategy. Namely, we set the initial conditions in (8) to zero and study the responses of the linearized dynamics to uncertain body forces. When the body forces are absent, the response of stable flows eventually decays to zero. However, in the presence of stochastic body forces, the linearized NS equations are capable of maintaining high levels of the steady-state variance [9]–[11]. Our analysis quantifies the effect of streamwise traveling waves on the asymptotic levels of variance and describes how sensitivity to background disturbances changes in the presence of control.

Let us assume that a stable system (8) is subject to a zero-mean white stochastic process (in y and t) $\mathbf{d}_\theta(y,k_z,t)$. Then, for each k_z and θ, the H_2 norm is determined by

$$\bar{\mathrm{E}}(\theta,k_z) \;=\; \mathrm{trace}\,(\lim_{t\to\infty}\mathcal{E}\,\{\mathbf{v}_\theta(\cdot,k_z,t)\otimes\mathbf{v}_\theta(\cdot,k_z,t)\}),$$

where $\mathcal{E}$ is the expectation operator and $\mathbf{v}_\theta\otimes\mathbf{v}_\theta$ is the tensor product of $\mathbf{v}_\theta$ with itself. We note that $\bar{\mathrm{E}}(\theta,k_z)$ determines the asymptotic level of variance maintained by a stochastic forcing in (8). Typically, this quantity is computed by running DNS of the NS equations until the statistical steady-state is reached. However, for linearized system (8), $\bar{\mathrm{E}}(\theta,k_z)$ can be determined using the solution to the following operator Lyapunov equation [12]

$$\mathcal{A}_\theta(k_z)\mathcal{X}_\theta(k_z) \;+\; \mathcal{X}_\theta(k_z)\mathcal{A}_\theta^*(k_z) \;=\; -\,\mathcal{B}_\theta(k_z)\mathcal{B}_\theta^*(k_z), \qquad (9)$$

as

$$\bar{\mathrm{E}}(\theta,k_z) \;=\; \mathrm{trace}\,(\mathcal{X}_\theta(k_z)\,\mathcal{C}_\theta^*(k_z)\,\mathcal{C}_\theta(k_z)).$$

Here, $\mathcal{X}_\theta(k_z)$ denotes the autocorrelation operator of $\boldsymbol{\psi}_\theta$, i.e., $\mathcal{X}_\theta(k_z) = \lim_{t\to\infty}\mathcal{E}\,\{\boldsymbol{\psi}_\theta(\cdot,k_z,t)\otimes\boldsymbol{\psi}_\theta(\cdot,k_z,t)\}$. Since $\mathcal{C}_\theta^*(k_z)\,\mathcal{C}_\theta(k_z)$ is an identity operator, we have

$$\bar{\mathrm{E}}(\theta,k_z) = \mathrm{trace}\,(\mathcal{X}_\theta(k_z)) = \sum_{n=-\infty}^{\infty}\mathrm{trace}\,(X_d(\theta_n,k_z)), \qquad (10)$$

where $X_d(\theta_n,k_z)$ denotes the elements on the main diagonal of operator $\mathcal{X}_\theta$.

D. Perturbation analysis of H_2 norm

Solving (9) is computationally expensive; a discretization of the operators (in y) and truncation of the bi-infinite matrices convert (9) into a large-scale matrix Lyapunov equation. Instead, we employ an efficient perturbation-analysis-based approach [13] for solving equation (9). This method is well-suited for systems with small amplitude spatially periodic terms and it converts (9) into a set of conveniently coupled system of operator-valued Lyapunov and Sylvester equations. A finite dimensional approximation of these equations yields a set of algebraic matrix equations whose order is determined by the number of fields in the evolution model (here 2, the wall-normal velocity and vorticity) times the size of discretization in y.

It can be shown that for $0 < \alpha \ll 1$, the H_2 norm of system (6) can be represented as

$$\begin{aligned}\bar{\mathrm{E}}(\theta,k_z;R_c,\alpha,c,\omega_x) \;=\; \bar{\mathrm{E}}_0(\theta,k_z;R_c,\omega_x) \;+\\ \alpha^2\,\bar{\mathrm{E}}_2(\theta,k_z;R_c,c,\omega_x) \;+\; \mathcal{O}(\alpha^4).\end{aligned} \qquad (11)$$

Thus, only terms with even powers in α contribute to $\bar{\mathrm{E}}$, which in controlled flow depends on six parameters. Since

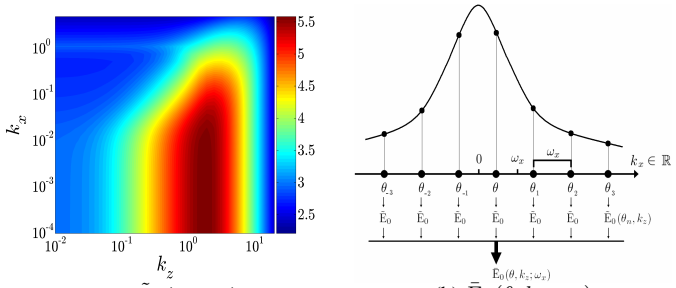

(a) $\tilde{\mathrm{E}}_0(k_x, k_z)$ (b) $\bar{\mathrm{E}}_0(\theta, k_z; \omega_x)$

Fig. 4. (a) The H_2 norm, $\tilde{\mathrm{E}}_0(k_x, k_z)$, of the uncontrolled channel flow with $R_c = 2000$. The plot is given in the log-log-log scale; and (b) For fixed ω_x and θ, $\bar{\mathrm{E}}_0(\theta, k_z; \omega_x)$ represents H_2 norm of fluctuations composed of all wavenumbers $\theta_n = \{\theta + n\omega_x\}_{n\in\mathbb{Z}}$; $\bar{\mathrm{E}}_0(\theta, k_z; \omega_x) = \sum_{n=-\infty}^{\infty} \tilde{\mathrm{E}}_0(\theta + n\omega_x, k_z)$.

our objective is to identify trends in the H_2 norm, we confine our attention to a perturbation analysis up to a second order in α. In § IV-C, we show that the essential trends are correctly predicted by the second order of correction.

IV. H_2 NORM IN CHANNEL FLOW WITH $R_c = 2000$

In this section, we study the H_2 norm of stochastically forced linearized NS equations in channel flows subject to streamwise traveling waves. Equation (11) reveals the dependence of the H_2 norm on traveling wave amplitude α, for $0 < \alpha \ll 1$. However, since the operators in (8) depend on the spatial wavenumbers (θ and k_z), R_c, ω_x, and c, the H_2 norm is also a function of these parameters. Finding the optimal triple (α, c, ω_x) that minimizes the H_2 norm is outside the scope of the current study; however, we identify the values of c and ω_x that are capable of reducing the H_2 norm in flows subject to small amplitude traveling waves, thereby providing guidelines for the selection of wave speed and frequency for controlling the onset of turbulence.

A. H_2 norm of uncontrolled flow

We briefly comment on the H_2 norm of the uncontrolled channel flow with $R_c = 2000$; for an in-depth treatment of this problem see [11]. The appropriate normal modes in the uncontrolled flow are purely harmonic streamwise and spanwise waves $\mathrm{e}^{\mathrm{i}k_x x}\,\mathrm{e}^{\mathrm{i}k_z z}$, where k_x denotes the streamwise wavenumber. Fig. 4(a) illustrates the H_2 norm of the uncontrolled flow as a function of k_x and k_z, which we denote by $\tilde{\mathrm{E}}_0(k_x, k_z)$. The streamwise constant fluctuations with $\mathcal{O}(1)$ spanwise wavenumbers carry most energy in the uncontrolled flow. Namely, the largest value of $\tilde{\mathrm{E}}_0(k_x, k_z)$ occurs at $(k_x = 0,\ k_z \approx 1.78)$. We note that these input-output resonances do not correspond to the least-stable modes of the linearized NS equation. Rather, they arise because of the coupling from the wall-normal velocity v to the wall-normal vorticity η. Physically, this coupling is a product of the vortex tilting (or lift-up) mechanism. On the other hand, the least-stable modes of uncontrolled flow create a local peak in $\tilde{\mathrm{E}}_0(k_x, k_z)$ around $(k_z = 0,\ k_x \approx 1.2)$, with a magnitude significantly lower compared to the magnitude achieved by the streamwise constant modes. Finally, the H_2 norm of the uncontrolled flow $\bar{\mathrm{E}}_0(\theta, k_z; \omega_x)$ as appeared in (11) can be obtained from $\bar{\mathrm{E}}_0(\theta, k_z; \omega_x) = \sum_{n=-\infty}^{\infty} \tilde{\mathrm{E}}_0(\theta + n\omega_x, k_z)$. In other words, for fixed ω_x and θ, $\bar{\mathrm{E}}_0(\theta, k_z; \omega_x)$ represents the H_2 norm of velocity fluctuations that are composed of all wavenumbers $k_x = \{\theta + n\omega_x\}_{n\in\mathbb{Z}}$. In comparison, $\tilde{\mathrm{E}}_0(k_x, k_z)$ is the H_2 norm of velocity fluctuations composed of a single wavenumber k_x (for illustration, see Fig. 4(b)).

B. Variance amplification of controlled flow

We next consider the H_2 norm of channel flow with $R_c = 2000$ in the presence of UTWs and DTWs. In flows subject to small amplitude blowing and suction along the walls, the perturbation analysis can be used to obtain an explicit formula for variance amplification (cf. (11))

$$\frac{\bar{\mathrm{E}}(\theta, k_z; \alpha, c, \omega_x)}{\bar{\mathrm{E}}_0(\theta, k_z; \omega_x)} \;\approx\; 1 + \alpha^2\, g_2(\theta, k_z; c, \omega_x). \qquad (12)$$

Thus, influence of control can be assessed by evaluating function $g_2 = \bar{\mathrm{E}}_2/\bar{\mathrm{E}}_0$ that quantifies variance amplification up to a second order in α. While the H_2 norm of the uncontrolled flow $\bar{\mathrm{E}}_0$ is always positive, the corrections to it (e.g., $\bar{\mathrm{E}}_2$) can assume both positive and negative values with vastly different magnitudes. It is thus advantageous to visualize function g_2 using a sign-preserving logarithmic scale

$$\hat{g}_2 \;=\; \mathrm{sign}(g_2)\log_{10}(1 + |g_2|).$$

For example, $\hat{g}_2 = 5$ or $\hat{g}_2 = -3$, respectively, signify $\bar{\mathrm{E}}_2 = 10^5\,\bar{\mathrm{E}}_0$ or $\bar{\mathrm{E}}_2 = -10^3\,\bar{\mathrm{E}}_0$.

Since most amplification in the uncontrolled flow occurs for fluctuations with $(k_x = 0,\ k_z = 1.78)$, it is relevant to study the influence of controls on these most energetic modes. In the controlled flow, the streamwise-constant modes are imbedded in the fundamental mode, i.e. fluctuations with $\theta = 0$ (cf. § III-B). As the plots of $\hat{g}_2$ in Figs. 5(a) and 5(b) reveal, the values of c and ω_x determine whether these modes are amplified or attenuated by the traveling waves. Up to a second order in α, the control parameters associated with the blue regions in these two figures reduce variance amplification of the uncontrolled flow. As evident from Fig. 5(a), only a narrow range of UTWs with $\omega_x \lesssim 0.1$ is capable of reducing variance amplification. However, since the required power for maintaining the nominal flow for such low frequency controls is prohibitively large, the choice of UTWs for transition control is not favorable from efficiency point of view. On the other hand, a large range of DTW parameters is capable of making a controlled flow less sensitive to stochastic excitations (cf. Fig. 5(b)). Moreover, our results show that the $\omega_x \gtrsim 0.1$ region contains the smallest required power for sustaining the DTWs; this suggests the potential of properly designed DTWs for maintaining a laminar flow with positive net efficiency (as confirmed by high fidelity simulations in [1]). It is noteworthy that traveling waves with parameters considered in [2] (i.e., $\omega_x = \{0.5, 1, 1.5, 2\}$ and $-4 < c < 0$) increase amplification of the most energetic modes of the uncontrolled flow (cf. Fig. 5(a)). Simulations of [1] show that such UTWs promote turbulence even for initial conditions for which the uncontrolled flow stays laminar.

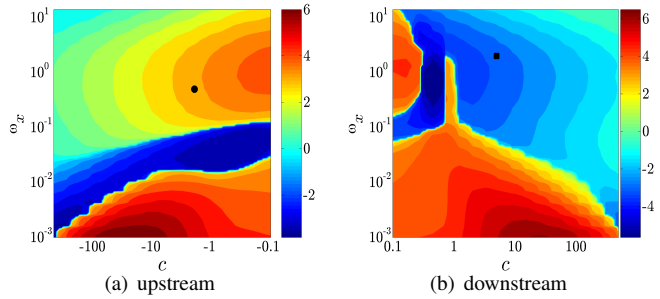

(a) upstream (b) downstream

Fig. 5. Second order correction to variance amplification, $\hat{g}_2(c, \omega_x)$, of the modes with $(\theta, k_z) = (0, 1.78)$, in the presence of (a) UTWs; and (b) DTWs in channel flow with $R_c = 2000$. The dot and the square, respectively, denote $(c = -2, \omega_x = 0.5)$ and $(c = 5, \omega_x = 2)$. The color plots are obtained using a sign-preserving logarithmic scale; e.g., $\hat{g}_2 = 5$ and $\hat{g}_2 = -3$ should be interpreted as $\bar{\mathrm{E}}_2 = 10^5\, \bar{\mathrm{E}}_0$ and $\bar{\mathrm{E}}_2 = -10^3\, \bar{\mathrm{E}}_0$.

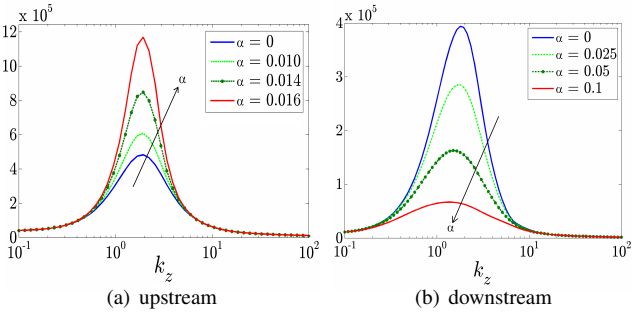

(a) upstream (b) downstream

Fig. 6. The H_2 norm, $\bar{\mathrm{E}}(k_z)$, of the fundamental mode $\theta = 0$ in channel flow with $R_c = 2000$ subject to: (a) a UTW with $c = -2$ and $\omega_x = 0.5$; and (b) a DTW with $c = 5$ and $\omega_x = 2$.

C. Effect of control amplitude on the H_2 norm

We next discuss influence of control amplitude on the H_2 norm. Our computations show that perturbation analysis (up to a second order in α) correctly predicts all essential trends. Fig. 6 compares the H_2 norm of the fundamental mode in uncontrolled channel flow with $R_c = 2000$ (blue curves), and in the controlled flows subject to: (a) a UTW with $c = -2$ and $\omega_x = 0.5$, Fig. 6(a); and (b) a DTW with $c = 5$ and $\omega_x = 2$, Fig. 6(b). The controlled flow results are obtained using large-scale truncation of the operators in Lyapunov equation (9). Fig. 6(b) shows that the properly designed DTWs with amplitudes equal to 5 %, 10 %, and 20 % of the base centerline velocity reduce the peak value of the H_2 norm of the uncontrolled flow by approximately 28 %, 60 %, and 80 %, respectively.

In contrast to DTWs, Fig. 6(a) demonstrates that the UTWs with $c = -2$ and $\omega_x = 0.5$ increase variance amplification. We note that all of these trends are correctly captured by the second order correction (in α) to the H_2 norm. Furthermore, the large H_2 norm caused by UTWs can be thought of as a precursor to flow instability; namely, it turns out that the UTWs destabilize the flow for $\alpha > 0.03$ which is a smaller value compared to the amplitudes chosen in [2] ($\alpha = 0.05$ and $\alpha = 0.125$, respectively). Therefore, the UTWs at best exhibit similar sensitivity to background disturbances as the uncontrolled flow. For control amplitudes shown in Fig. 6, we have verified stability of fluctuations around base velocities in both UTWs and DTWs by computing the eigenvalues of the large-scale truncation of operator $\mathcal{A}_\theta(k_z)$ in (8).

V. Concluding Remarks

We have used input-output analysis of the linearized NS equation to examine the effect of traveling waves on the dynamics of velocity fluctuations in a transitional channel flow. Our simulation-free design employs perturbation analysis as a basis for identification of the traveling wave frequencies and speeds that are capable of reducing variance amplification in the presence of small amplitude actuation. Contrary to current practice, this approach avoids the need for extensive numerical simulations and experiments in the early design stages.

Our results indicate that the UTWs are poor candidates for preventing transition as they amplify the most energetic modes of the uncontrolled flow. On the contrary, the properly designed DTWs can significantly reduce the variance amplification of 3D fluctuations, which makes them well-suited for controlling the onset of turbulence. In addition, we have studied the net power balance of flows subject to traveling waves. The predictive power of our approach is demonstrated in a companion paper [1] where all theoretical findings are confirmed by numerical simulations of the nonlinear NS equations. In particular, the DTWs identified by our analysis can maintain a laminar flow and achieve a positive net efficiency relative to the uncontrolled flow that becomes turbulent.

References

[1] B. K. Lieu, R. Moarref, and M. R. Jovanović, "Preventing transition to turbulence using streamwise traveling waves: direct numerical simulations," in *Proceedings of the 2010 American Control Conference*, Baltimore, MD, 2010, to appear.

[2] T. Min, S. M. Kang, J. L. Speyer, and J. Kim, "Sustained sub-laminar drag in a fully developed channel flow," *J. Fluid Mech.*, vol. 558, pp. 309–318, 2006.

[3] T. R. Bewley, "A fundamental limit on the balance of power in a transpiration-controlled channel flow," *J. Fluid Mech.*, vol. 632, pp. 443–446, 2009.

[4] J. Hœpffner and K. Fukagata, "Pumping or drag reduction?" *J. Fluid Mech.*, vol. 635, pp. 171–187, 2009.

[5] I. G. Currie, *Fundamental Mechanics of Fluids*. CRC Press, 2003.

[6] M. Quadrio and P. Ricco, "Critical assessment of turbulent drag reduction through spanwise wall oscillations," *J. Fluid Mech.*, vol. 521, pp. 251–271, 2004.

[7] A. H. Nayfeh and D. T. Mook, *Nonlinear oscillations*. New York: John Wiley & Sons, 1979.

[8] P. J. Schmid, "Nonmodal stability theory," *Annu. Rev. Fluid Mech.*, vol. 39, pp. 129–162, 2007.

[9] B. F. Farrell and P. J. Ioannou, "Stochastic forcing of the linearized Navier-Stokes equations," *Phys. Fluids A*, vol. 5, no. 11, pp. 2600–2609, 1993.

[10] B. Bamieh and M. Dahleh, "Energy amplification in channel flows with stochastic excitation," *Phys. Fluids*, vol. 13, no. 11, pp. 3258–3269, 2001.

[11] M. R. Jovanović and B. Bamieh, "Componentwise energy amplification in channel flows," *J. Fluid Mech.*, vol. 534, pp. 145–183, July 2005.

[12] M. Fardad, M. R. Jovanović, and B. Bamieh, "Frequency analysis and norms of distributed spatially periodic systems," *IEEE Trans. Automat. Control*, vol. 53, no. 10, pp. 2266–2279, November 2008.

[13] M. Fardad and B. Bamieh, "Perturbation methods in stability and norm analysis of spatially periodic systems," *SIAM J. Control Optim.*, vol. 47, no. 2, pp. 997–1021, 2008.